Chapter 13

Ultrafast and Intense-Field Nonlinear Optics

13.1 Introduction

There is currently great interest in the physics of ultrashort laser pulses. Recent advances have led to the generation of laser pulses with durations of the order of 1 attosecond (Hentschel et al., 2001). Ultrashort pulses can be used to probe the properties of matter on extremely short time scales. Within the context of nonlinear optics, ultrashort laser pulses are of interest for at least two separate reasons. The first reason is that the nature of nonlinear optical interactions is often profoundly modified through the use of ultrashort laser pulses, in part because of the broad spectral bandwidth necessarily associated with such pulses. The next two sections of this chapter treat various aspects of the resulting modifications of the nature of nonlinear optical interactions. The second reason is that ultrashort laser pulses tend to possess extremely high peak intensities (because laser pulse energies tend to be established by the energy-storage capabilities of laser gain media), and thus short laser pulses tend to have much higher peak powers than longer pulses. The second half of this chapter is devoted to a survey of the sorts of nonlinear optical processes that can be excited by extremely intense laser fields.

13.2 Ultrashort-Pulse Propagation Equation

In this section and the following, we treat aspects of the propagation of ultrashort laser pulses through optical systems. Some physical processes that will be included in this analysis include the influence of high-order dispersion, space–time coupling effects, and self-steepening leading to the formation of optical shock waves. In the present section we derive a form of the pulse-propagation equation relevant to the propagation of an ultrashort laser pulse through a dispersive, nonlinear optical medium. In many ways, this equation can be considered to be a generalization of the pulse-propagation equation (the so-called nonlinear Schrödinger equation)

Nonlinear Optics. https://doi.org/10.1016/B978-0-12-811002-7.00022-9

of Section 7.5. To derive this generalized equation, we begin with the wave equation in the time domain (see, for instance, Eq. (2.1.15)) which we express as

$$\nabla^2 \tilde{E}(\mathbf{r},t) - \frac{1}{\epsilon_0 c^2}\frac{\partial^2 \tilde{D}^{(1)}(\mathbf{r},t)}{\partial t^2} = \frac{1}{\epsilon_0 c^2}\frac{\partial^2 \tilde{P}(\mathbf{r},t)}{\partial t^2}. \tag{13.2.1}$$

We express the field quantities in terms of their Fourier transforms as

$$\tilde{E}(\mathbf{r},t) = \int E(\mathbf{r},\omega)e^{-i\omega t}d\omega/2\pi, \tag{13.2.2a}$$

$$\tilde{D}^{(1)}(\mathbf{r},t) = \int D^{(1)}(\mathbf{r},\omega)e^{-i\omega t}d\omega/2\pi, \tag{13.2.2b}$$

$$\tilde{P}(\mathbf{r},t) = \int P(\mathbf{r},\omega)e^{-i\omega t}d\omega/2\pi, \tag{13.2.2c}$$

where all of the integrals are to be performed over the range $-\infty$ to ∞. We assume that $D^{(1)}(\mathbf{r},\omega)$ and $E(\mathbf{r},\omega)$ are related by the usual linear dispersion relation as

$$D^{(1)}(\mathbf{r},\omega) = \epsilon_0 \epsilon^{(1)}(\omega)E(\mathbf{r},\omega) \tag{13.2.3}$$

and that $\tilde{P}$ represents the nonlinear part of the material response. By introducing these forms into Eq. (13.2.1), we obtain a relation that can be regarded as the wave equation in the frequency domain, and which is given by

$$\nabla^2 E(\mathbf{r},\omega) + \epsilon^{(1)}(\omega)(\omega^2/c^2)E(\mathbf{r},\omega) = -(\omega^2/\epsilon_0 c^2)P(\mathbf{r},\omega). \tag{13.2.4}$$

Our goal is to derive a wave equation for the slowly varying field amplitude $\tilde{A}(\mathbf{r},t)$ defined by

$$\tilde{E}(\mathbf{r},t) = \tilde{A}(\mathbf{r},t)\, e^{i(k_0 z - \omega_0 t)} + \text{c.c.}, \tag{13.2.5}$$

where ω_0 is the central frequency of the pulse and $k_0 = [\epsilon^{(1)}(\omega_0)]^{1/2}\omega_0/c$ is the linear portion of the wavevector magnitude at this frequency. We represent $\tilde{A}(\mathbf{r},t)$ in terms of its spectral content as

$$\tilde{A}(\mathbf{r},t) = \int A(\mathbf{r},\omega)\, e^{-i\omega t}d\omega/2\pi. \tag{13.2.6}$$

Note that $E(\mathbf{r},\omega)$ and $A(\mathbf{r},\omega)$ are related as in Eq. (7.5.16) by

$$E(\mathbf{r},\omega) \simeq A(\mathbf{r},\omega-\omega_0)e^{ik_0 z}. \tag{13.2.7}$$

In terms of the quantity $A(\mathbf{r},\omega)$ (the slowly varying field amplitude in the frequency domain) the wave equation (13.2.4) becomes

$$\left[\nabla_\perp^2 + \frac{\partial^2}{\partial z^2} + 2ik_0\frac{\partial}{\partial z} + \left[k^2(\omega) - k_0^2\right]\right]A(\mathbf{r},\omega) = -\frac{\omega^2}{\epsilon_0 c^2}P(\mathbf{r},\omega)e^{-ik_0 z} \tag{13.2.8}$$

where we have introduced

$$k^2(\omega) = \epsilon^{(1)}(\omega)(\omega^2/c^2). \tag{13.2.9}$$

We next approximate $k(\omega)$ as a power series in the frequency difference $\omega - \omega_0$ as

$$k(\omega) = k_0 + (\omega - \omega_0)k_1(\omega_0) + D(\omega) \tag{13.2.10a}$$

where

$$D(\omega) = \sum_{n=2}^{\infty} \frac{1}{n!}(\omega - \omega_0)^n k_n(\omega_0) \tag{13.2.10b}$$

and where $k_n(\omega_0) = d^n k(\omega)/d\omega^n$, evaluated at $\omega = \omega_0$. We thus express $k^2(\omega)$ as

$$\begin{aligned} k^2(\omega) &= k_0^2 + 2(\omega - \omega_0)k_1 k_0 \\ &+ 2k_0 D(\omega) + 2(\omega - \omega_0)k_1 D(\omega) + (\omega - \omega_0)^2 k_1^2 + D^2(\omega). \end{aligned} \tag{13.2.11}$$

Here $D(\omega)$ represents high-order dispersion. We have displayed explicitly the linear term $k_1(\omega - \omega_0)$ in the power series expansion because k_1 has a direct physical interpretation as the inverse of the group velocity. We now introduce this expression into the wave equation in the form of Eq. (13.2.8), which then becomes

$$\begin{aligned} &\left[\nabla_\perp^2 + \frac{\partial^2}{\partial z^2} + 2ik_0\frac{\partial}{\partial z} + 2(\omega - \omega_0)k_0 k_1 + 2k_0 D + 2(\omega - \omega_0)k_1 D \right. \\ &\left. + (\omega - \omega_0)^2 k_1^2\right] A(\mathbf{r}, \omega) = \left(\omega^2/\epsilon_0 c^2\right) P(z, \omega) e^{-ik_0 z}, \end{aligned} \tag{13.2.12}$$

where we have dropped the contribution $D(\omega)^2$ because it is invariably small. We now convert this equation back to the time domain. To do so, we multiply each term of the equation by $\exp[-i(\omega - \omega_0)t]$ and integrate over all values of $\omega - \omega_0$. We obtain

$$\begin{aligned} &\left[\nabla_\perp^2 + \frac{\partial^2}{\partial z^2} + 2ik_0\left(\frac{\partial}{\partial z} + k_1\frac{\partial}{\partial t}\right) + 2ik_1\tilde{D}\frac{\partial}{\partial t} + 2k_0\tilde{D} - k_1^2\frac{\partial^2}{\partial t^2}\right]\tilde{A}(\mathbf{r}, t) \\ &\quad = -\frac{1}{\epsilon_0 c^2}\frac{\partial^2 \tilde{P}}{\partial t^2} e^{-i(k_0 z - \omega_0 t)}, \end{aligned} \tag{13.2.13}$$

where $\tilde{D}$ represents the differential operator

$$\tilde{D} = \sum_{n=2}^{\infty} \frac{1}{n!} k_n \left(i\frac{\partial}{\partial t}\right)^n = -\frac{1}{2}k_2\frac{\partial^2}{\partial t^2} - \frac{i}{6}k_3\frac{\partial^3}{\partial t^3} + \cdots. \tag{13.2.14}$$

We next examine the form of the right-hand side of this equation. We represent the time-domain polarization in terms of its slowly varying amplitude (slowly varying in space and time)* $\tilde{p}(\mathbf{r}, t)$ as

$$\tilde{P}(\mathbf{r}, t) = \tilde{p}(\mathbf{r}, t) e^{i(k_0 z - \omega_0 t)} + \text{c.c.} \tag{13.2.16}$$

We thus find that

$$\begin{aligned} \frac{\partial \tilde{P}}{\partial t} &= \left(-i\omega_0 \tilde{p} + \frac{\partial \tilde{p}}{\partial t} \right) e^{i(k_0 z - \omega_0 t)} + \text{c.c.} \\ &= -i\omega_0 \left[\left(1 + \frac{i}{\omega_0} \frac{\partial}{\partial t} \right) \tilde{p} \right] e^{i(k_0 z - \omega_0 t)} + \text{c.c.} \end{aligned} \tag{13.2.17a}$$

and

$$\frac{\partial^2 \tilde{P}}{\partial t^2} = -\omega_0^2 \left[\left(1 + \frac{i}{\omega_0} \frac{\partial}{\partial t} \right)^2 \tilde{p} \right] e^{i(k_0 z - \omega_0 t)} + \text{c.c.} \tag{13.2.17b}$$

By introducing this expression into the wave equation in the form (13.2.13), we obtain

$$\begin{aligned} &\left[\nabla_\perp^2 + \frac{\partial^2}{\partial z^2} + 2ik_0 \left(\frac{\partial}{\partial z} + k_1 \frac{\partial}{\partial t} \right) + 2k_0 \tilde{D} + 2ik_1 \tilde{D} \frac{\partial}{\partial t} - k_1^2 \frac{\partial^2}{\partial t^2} \right] \tilde{A}(\mathbf{r}, t) \\ &\quad = -\frac{\omega_0^2}{\epsilon_0 c^2} \left(1 + \frac{i}{\omega_0} \frac{\partial}{\partial t} \right)^2 \tilde{p}(\mathbf{r}, t) \,. \end{aligned} \tag{13.2.18}$$

Next we convert this equation to a retarded time frame specified by the coordinates z' and τ defined by

$$z' = z \qquad \text{and} \qquad \tau = t - \frac{1}{v_g} z = t - k_1 z, \tag{13.2.19}$$

so that (see also Eq. (7.5.29) for a somewhat different development)

$$\frac{\partial}{\partial z} = \frac{\partial}{\partial z'} - k_1 \frac{\partial}{\partial \tau} \qquad \text{and} \qquad \frac{\partial}{\partial t} = \frac{\partial}{\partial \tau}. \tag{13.2.20}$$

* For example, for the case of a material with an instantaneous third-order response, the polarization amplitude is given by

$$\tilde{p}(\mathbf{r}, t) = \epsilon_0 \chi^{(3)} |\tilde{A}(\mathbf{r}, t)|^2 \tilde{A}(\mathbf{r}, t) \,. \tag{13.2.15}$$

In this new reference frame, the wave equation becomes

$$\left[\nabla_\perp^2 + \frac{\partial^2}{\partial z'^2} - 2k_1\,\frac{\partial}{\partial z'}\frac{\partial}{\partial \tau} + k_1^2\frac{\partial^2}{\partial \tau^2} + 2ik_0\left(\frac{\partial}{\partial z'} - k_1\frac{\partial}{\partial \tau} + k_1\frac{\partial}{\partial \tau}\right)\right.$$
$$\left. + 2k_0\tilde{D} + 2ik_1\tilde{D}\frac{\partial}{\partial \tau} - k_1^2\frac{\partial^2}{\partial \tau^2}\right]\tilde{A}(\mathbf{r},\tau) = \tag{13.2.21}$$
$$-\frac{\omega_0^2}{\epsilon_0 c^2}\left(1 + \frac{i}{\omega_0}\frac{\partial}{\partial \tau}\right)^2 \tilde{p}(\mathbf{r},\tau)\,.$$

We now drop the term $\partial^2/\partial z'^2$ by arguing that it is much smaller than $k_0\,\partial/\partial z'$. This approximation is conventionally known as the slowly varying amplitude (or envelope) approximation (see for example Eq. (2.2.9)), but especially in the present context it might better be called the slowly evolving wave approximation in that it entails the spatial and not the temporal evolution of the field amplitude. The resulting equation then becomes

$$\left[\nabla_\perp^2 - 2k_1\frac{\partial}{\partial z'}\frac{\partial}{\partial \tau} + 2ik_0\frac{\partial}{\partial z'} + 2k_0\tilde{D} + 2ik_1\tilde{D}\frac{\partial}{\partial \tau}\right]\tilde{A}(\mathbf{r},\tau)$$
$$= -\frac{\omega_0^2}{\epsilon_0 c^2}\left(1 + \frac{i}{\omega_0}\frac{\partial}{\partial \tau}\right)^2 \tilde{p}(\mathbf{r},\tau)\,. \tag{13.2.22}$$

This equation can alternatively be written as

$$\left[\nabla_\perp^2 + 2ik_0\frac{\partial}{\partial z'}\left(1 + \frac{ik_1}{k_0}\frac{\partial}{\partial \tau}\right) + 2k_0\tilde{D}\left(1 + \frac{ik_1}{k_0}\frac{\partial}{\partial \tau}\right)\right]\tilde{A}\,(\mathbf{r},\tau)$$
$$= -\frac{\omega_0^2}{\epsilon_0 c^2}\left(1 + \frac{i}{\omega_0}\frac{\partial}{\partial \tau}\right)^2 \tilde{p}(\mathbf{r},\tau)\,. \tag{13.2.23}$$

Note that two of the terms in this equation depend on the ratio k_1/k_0. This ratio can be evaluated as follows: $k_1/k_0 = v_g^{-1}/(n_0\omega_0/c) = n_g/(n_0\omega_0)$, where we have introduced the group index $n_g = c/v_g$. We now ignore the effects of dispersion in evaluating this ratio, that is, we set n_g equal to n so that the ratio is given by $k_1/k_0 = 1/\omega_0$. Note that we have otherwise retained the effects of dispersion on the overall propagation of the pulse by means of the quantity $\tilde{D}$. It is believed that the effects of dispersion on the ratio k_1/k_0 are higher-order effects and can therefore be neglected. In this approximation the wave equation becomes

$$\left[\nabla_\perp^2 + 2ik_0\frac{\partial}{\partial z'}\left(1 + \frac{i}{\omega_0}\frac{\partial}{\partial \tau}\right) + 2k_0\tilde{D}\left(1 + \frac{i}{\omega_0}\frac{\partial}{\partial \tau}\right)\right]\tilde{A}\,(\mathbf{r},\tau)$$
$$= -\frac{\omega_0^2}{\epsilon_0 c^2}\left(1 + \frac{i}{\omega_0}\frac{\partial}{\partial \tau}\right)^2 \tilde{p}(\mathbf{r},\tau), \tag{13.2.24}$$

which can also be expressed as

$$\left[\left(1+\frac{i}{\omega_0}\frac{\partial}{\partial\tau}\right)^{-1}\nabla_\perp^2+2ik_0\frac{\partial}{\partial z'}+2k_0\tilde{D}\right]\tilde{A}(\mathbf{r},\tau)$$
$$=-\frac{\omega_0^2}{\epsilon_0 c^2}\left(1+\frac{i}{\omega_0}\frac{\partial}{\partial\tau}\right)\tilde{p}(\mathbf{r},\tau). \tag{13.2.25}$$

This equation, in either form, is known as the envelope equation* or as the ultrashort-pulse propagation equation. It was first obtained by Brabec and Krausz (1997), and thus is also known as the Brabec–Krausz equation. It can be considered to be a generalization of the usual nonlinear Schrödinger equation (7.5.32) in that it includes the effects of high-order dispersion (through the term that includes $\tilde{D}$), space–time coupling (through the presence of the differential operator $\partial/\partial\tau$ on the left-hand side of the equation), and self-steepening (through the presence of the differential operator $\partial/\partial\tau$ on the right-hand side). This equation is believed to be accurate in describing the propagation of pulses as short as one optical cycle in duration. We recall that this equation is valid only within the slowly evolving wave and paraxial approximations. It can be used to treat many types of nonlinear response. For instance, for a material displaying an instantaneous third- and fifth-order nonlinearity, $\tilde{p}$ is given by $\tilde{p}=\epsilon_0\chi^{(3)}|\tilde{A}|^2\tilde{A}+\epsilon_0\chi^{(5)}|\tilde{A}|^4\tilde{A}$.

These envelope equations can also be used to treat a material possessing a dispersive nonlinear optical response. For ultrashort laser pulses, the value of $\chi^{(3)}$ can vary appreciably for different frequency components of the pulse. The effects of the dispersion of $\chi^{(3)}$ can be modeled in lowest approximation (see for instance Diels and Rudolph, 1996, p. 139) by representing $\chi^{(3)}(\omega)\equiv\chi^{(3)}(\omega=\omega+\omega-\omega)$ as

$$\chi^{(3)}(\omega)=\chi^{(3)}(\omega_0)+(\omega-\omega_0)\frac{d\chi^{(3)}}{d\omega}, \tag{13.2.26}$$

where the derivative is to be evaluated at frequency ω_0. Thus $p(\omega)$ can be expressed as

$$p(\omega)=3\epsilon_0\left[\chi^{(3)}(\omega_0)+(\omega-\omega_0)\frac{d\chi^{(3)}}{d\omega}\right]|A(\omega)|^2A(\omega). \tag{13.2.27}$$

This relation can be converted to the time domain through use of the same procedure used in going from Eq. (13.2.12) to Eq. (13.2.13). One finds that

$$\tilde{p}(\mathbf{r},\tau)=3\epsilon_0\left[\chi^{(3)}(\omega_0)+\frac{d\chi^{(3)}}{d\omega}i\frac{\partial}{\partial\tau}\right]|\tilde{A}(\mathbf{r},\tau)|^2\tilde{A}(\mathbf{r},\tau). \tag{13.2.28}$$

* Eqs. (13.2.24) and (13.2.25) are known as envelope equations because they describe the propagation of the field envelope $\tilde{A}(\mathbf{r},t)$. Of course, the nonlinear Schrödinger equation in the form of Eq. (7.5.32) is also an envelope equation, although many authors reserve the name envelope equation for Eqs. (13.2.24) and (13.2.25) or their generalizations.

Here we have approximated the Fourier transform of $|\tilde{A}(\mathbf{r},\tau)|^2\tilde{A}(\mathbf{r},\tau)$ as $|A(\omega)|^2A(\omega)$. This expression for $\tilde{p}$ can be used directly in any of Eqs. (13.2.22) through (13.2.25). We consider Eq. (13.2.24). However, since Eq. (13.2.26) contains only a linear correction term in $(\omega-\omega_0)$, and consequently Eq. (13.2.28) contains only a contribution first-order in $\partial/\partial\tau$, for reasons of consistency one wants to include in the resulting pulse-propagation equation only contributions first-order in $\partial/\partial\tau$. Noting that

$$\left(1+\frac{i}{\omega_0}\frac{\partial}{\partial\tau}\right)^2=\left(1+\frac{2i}{\omega_0}\frac{\partial}{\partial\tau}-\frac{1}{\omega_0^2}\frac{\partial^2}{\partial\tau^2}\right)\approx\left(1+\frac{2i}{\omega_0}\frac{\partial}{\partial\tau}\right), \tag{13.2.29}$$

one finds that in this approximation the ultrashort-pulse propagation equation becomes

$$\left[\nabla_\perp^2+2ik_0\frac{\partial}{\partial z'}\left(1+\frac{i}{\omega_0}\frac{\partial}{\partial\tau}\right)+2k_0\tilde{D}\left(1+\frac{i}{\omega_0}\frac{\partial}{\partial\tau}\right)\right]\tilde{A}(\mathbf{r},\tau)$$
$$=(-3/c^2)\,\omega_0^2\,\chi^{(3)}(\omega_0)\left[1+\left(2+\frac{\omega_0}{\chi^{(3)}(\omega_o)}\frac{d\chi^{(3)}}{d\omega}\right)\frac{i}{\omega_0}\frac{\partial}{\partial\tau}\right]|\tilde{A}(\mathbf{r},\tau)|^2\tilde{A}(\mathbf{r},\tau). \tag{13.2.30}$$

This equation is a generalization of Eq. (13.2.24) in that it allows for dispersion in $\chi^{(3)}(\omega)$, but it is an approximation in that it includes only terms that are first order in $\partial/\partial\tau$. Procedures for incorporating other sorts of nonlinearities into the present formalism have been described by Gaeta (2000).

13.3 Interpretation of the Ultrashort-Pulse Propagation Equation

Let us now attempt to obtain some intuitive understanding of the various physical processes described by the ultrashort pulse propagation equation. For definiteness, we use the form of Eq. (13.2.24). As a first step, we study a simplified version of this equation obtained by ignoring the correction terms $(i/\omega_0)\partial/\partial\tau$ by replacing the factors $\left[1+(i/\omega_0)(\partial/\partial\tau)\right]$ by unity and by including only the lowest-order contribution (known as second-order dispersion) to $\tilde{D}$. One obtains

$$\frac{\partial\tilde{A}(\mathbf{r},\tau)}{\partial z'}=\left[\frac{i}{2k_0}\nabla_\perp^2-\frac{i}{2}\,k_2\frac{\partial^2}{\partial\tau^2}+\frac{3i\omega_0}{2n_0c}\chi^{(3)}(\omega_0)\,|\tilde{A}(\mathbf{r},\tau)|^2\right]\tilde{A}(\mathbf{r},\tau). \tag{13.3.1}$$

Written in this form, the equation leads to the interpretation that the field amplitude A varies with propagation distance z' (the left-hand side) because of three physical effects (the three terms on the right-hand side). The term involving the transverse Laplacian describes the spreading of the beam as a consequence of diffraction, the term involving the second time derivative describes the temporal spreading of the pulse as a consequence of group velocity dispersion,

and the third term describes the nonlinear acquisition of phase. It is useful to introduce distance scales over which each of the terms becomes appreciable. We define these scales as follows:

$$L_{\text{dif}} = \tfrac{1}{2}\, k_0 w_0^2 \qquad \text{(diffraction length)}, \tag{13.3.2a}$$

$$L_{\text{dis}} = T^2/|k_2| \qquad \text{(dispersion length)}, \tag{13.3.2b}$$

$$L_{\text{NL}} = \frac{2n_0 c}{3\omega_0 \chi^{(3)} |A|^2} = \frac{1}{(\omega_0/c) n_2 I} \qquad \text{(nonlinear length)}. \tag{13.3.2c}$$

In these equations w_0 is a measure of the characteristic beam radius, and T is a measure of the characteristic pulse duration. The significance of these distance scales is that for a given physical situation the process with the shortest distance scales is expected to be dominant. For reference, we note that the optical constants for fused silica at a wavelength of 800 nm are given by $n_2 = 3.5 \times 10^{-20}$ m^2/W and $k_2 = 446$ fsec^2/cm = 4.46 fsec^2/m. Through use of Eq. (13.3.2b), for example, we see that for a 20-fsec pulse propagating through fused silica L_{dis} is approximately 0.9 cm. Thus in propagating through 0.9 cm of fused silica a 20-fsec pulse approximately doubles in pulse duration as a consequence of group velocity dispersion.

13.3.1 Self-Steepening

Let us next examine the influence of the correction factor $\left[1 + (i/\omega_0)\,(\partial/\partial\tau)\right]$ on the nonlinear source term of Eq. (13.2.25). To isolate this influence, we drop the correction factor in other places in the equation. Also, to include the effects of the dispersion of $\chi^{(3)}$, we use the ultrashort pulse propagation equation in the form given by (13.2.30). We also transform back to the laboratory reference frame z, t (not the z', τ frame in which the pulse is nearly stationary) so that the factor $k_1 \partial\tilde{A}/\partial t = (1/v_g)\partial\tilde{A}/\partial t = (n_0^{(g)}/c)\partial\tilde{A}/\partial t$ appears explicitly in the wave equation, which takes the form

$$\begin{aligned}\frac{\partial\tilde{A}}{\partial z} + \frac{n_0^{(g)}}{c}\frac{\partial\tilde{A}}{\partial t} &= \frac{i}{2k_0}\nabla_\perp^2\tilde{A} - \frac{i}{2}k_2\frac{\partial^2\tilde{A}}{\partial t^2} + \frac{i3\omega_0}{2n_0 c}\chi^{(3)}(\omega_0)|\tilde{A}|^2\tilde{A} \\ &\quad + \frac{i3\omega_0}{2n_0 c}\chi^{(3)}(\omega_0)\left(2 + \frac{\omega_0}{\chi^{(3)}(\omega_0)}\frac{d\chi^{(3)}}{d\omega}\right)\frac{i}{\omega_0}\frac{\partial}{\partial t}\,|\tilde{A}|^2 A.\end{aligned} \tag{13.3.3}$$

We now introduce nonlinear coefficients γ_1 and γ_2 defined by

$$\gamma_1 = \frac{3\omega_0}{2n_0 c}\chi^{(3)}(\omega_0) \quad \text{and} \quad \gamma_2 = \frac{3\omega_0}{2n_0 c}\chi^{(3)}(\omega_0)\left(1 + \frac{1}{2}\frac{\omega_0}{\chi^{(3)}}\frac{d\chi^{(3)}}{d\omega}\right). \tag{13.3.4}$$

Note that in the absence of dispersion of the nonlinear susceptibility the nonlinear coefficients γ_1 and γ_2 are equal. In terms of these quantities, Eq. (13.3.3) can be expressed more concisely

as

$$\frac{\partial \tilde{A}}{\partial z} + \frac{n_0^{(g)}}{c}\frac{\partial \tilde{A}}{\partial t} = \frac{i}{2k_0}\nabla_\perp^2 \tilde{A} - \frac{i}{2}k_2\frac{\partial^2 \tilde{A}}{\partial t^2} + i\gamma_1|A|^2 A - 2\gamma_2\frac{1}{\omega_0}\frac{\partial}{\partial t}(|\tilde{A}|^2 A). \tag{13.3.5}$$

Next we note that the time derivative in the last term can be written as

$$\begin{aligned}\frac{\partial}{\partial t}(|\tilde{A}|^2\tilde{A}) &= \frac{\partial}{\partial t}(\tilde{A}^2\tilde{A}^*) = \tilde{A}^2\frac{\partial \tilde{A}^*}{\partial t} + 2\tilde{A}^*\tilde{A}\frac{\partial \tilde{A}}{\partial t} \\ &= 2|\tilde{A}|^2\frac{\partial \tilde{A}}{\partial t} + \tilde{A}^2\frac{\partial \tilde{A}^*}{\partial t}.\end{aligned} \tag{13.3.6}$$

The first contribution to the last form can be identified as an intensity-dependent contribution to the group velocity. The second contribution does not have a simple physical interpretation, but can be considered to represent a dispersive four-wave mixing term. To proceed, we make use of Eq. (13.3.6) to express Eq. (13.3.5) as

$$\frac{\partial \tilde{A}}{\partial z} + \frac{n_{\text{eff}}^{(g)}}{c}\frac{\partial \tilde{A}}{\partial t} = \frac{i}{2k_0}\nabla_\perp^2 \tilde{A} - \frac{i}{2}k_2\frac{\partial^2 \tilde{A}}{\partial t^2} + i\gamma_1|A|^2 A - \frac{2\gamma_2}{\omega_0}\tilde{A}^2\frac{\partial \tilde{A}^*}{\partial t} \tag{13.3.7}$$

where

$$n_{\text{eff}}^{(g)} = n_0^{(g)} + \frac{4\gamma_2 c}{\omega_0}|\tilde{A}|^2 \equiv n_0^{(g)} + n_2^{(g)} I. \tag{13.3.8}$$

In the last form of this relation, we have introduced the coefficient of the intensity dependence of the group index as

$$n_2^{(g)} = \frac{3}{n_0^2\epsilon_0 c}\chi^{(3)}(\omega_0)\left[1 + \frac{1}{2}\frac{\omega_0}{\chi^{(3)}(\omega_0)}\frac{d\chi^{(3)}}{d\omega}\right]. \tag{13.3.9}$$

Through use of Eq. (4.1.19), we see that this expression can be rewritten as

$$n_2^{(g)} = 4n_2\left[1 + \frac{1}{2}\frac{\omega_0}{\chi^{(3)}(\omega_0)}\frac{d\chi^{(3)}}{d\omega}\right]. \tag{13.3.10}$$

We thus see that the last term in Eq. (13.3.4) leads to an intensity dependence of the group index n_g as well as to the last term of Eq. (13.3.7), which as mentioned above is a dispersive four-wave mixing contribution. We also see from Eq. (13.3.9) that the intensity dependence of the group index depends both on the susceptibility itself and on its dispersion.

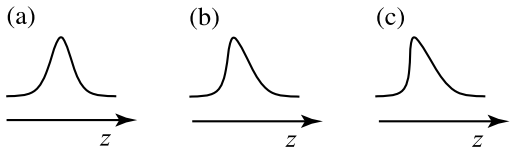

FIGURE 13.3.1: Self-steepening and optical shock-wave formation. (a) The incident optical pulse is assumed to have a Gaussian time evolution. (b) After propagation through a nonlinear medium, the pulse displays self-steepening, typically on its trailing edge. (c) If the self-steepening becomes sufficiently pronounced that the intensity changes instantaneously, an optical shock wave is formed.

The intensity dependence of the group velocity leads to the phenomena of self-steepening and optical shock wave formation. These phenomena are illustrated in Fig. 13.3.1. Note that for the usual situation in which $n_2^{(g)}$ is positive, the peak of the pulse is slowed down more than the edges of the pulse, leading to steepening of the trailing edge of the pulse. If this edge becomes infinitely steep, it is said to form an optical shock wave. Self-steepening has been described by DeMartini et al. (1967), by Yang and Shen (1984), and by Gaeta (2000). Note also that we can define a self-steepening distance scale analogous to these of Eqs. (13.3.2) by

$$L_{\rm ss} = \frac{cT}{n_2^{(g)} I}. \tag{13.3.11}$$

For the usual situation in which $n_2^{(g)} \approx n_2$, $L_{\rm ss}$ is much larger than $L_{\rm NL}$ (because, except for extremely short pulses, $cT \gg 1/k_0$), and thus self-steepening tends to be difficult to observe.

13.3.2 Space–Time Coupling

Let us now examine the influence of space–time coupling, that is, the influence of the differential operator $\left[1 + (i/\omega_0)\,\partial/\partial\tau\right]^{-1}$ on the left-hand side of Eq. (13.2.25). We can see the significance of this effect most simply by considering propagation through a dispersionless, linear material so that the wave equation becomes

$$\left(1 + \frac{i}{\omega_0}\frac{\partial}{\partial\tau}\right)^{-1} \nabla_\perp^2 \tilde{A}(\mathbf{r},\tau) + 2ik_0 \frac{\partial}{\partial z'}\tilde{A}(\mathbf{r},\tau) = 0. \tag{13.3.12}$$

The first term is said to represent space–time coupling because it involves both temporal and spatial derivatives of the field amplitude. To examine the significance of this mathematical form, it is useful to write this equation as

$$\nabla_\perp^2 \tilde{A}(\mathbf{r},\tau) + \left(1 + \frac{i}{\omega_0}\frac{\partial}{\partial\tau}\right) 2ik_0 \frac{\partial}{\partial z'}\tilde{A}(\mathbf{r},\tau) = 0. \tag{13.3.13}$$

Let us first consider the somewhat artificial example of a field of the form $\tilde{A}(\mathbf{r}, \tau) = a(\mathbf{r})e^{-i\delta\omega\tau}$; such a field is a monochromatic wave at frequency $\omega_0 + \delta\omega$. We substitute this form into Eq. (13.3.13) and obtain

$$\nabla_\perp^2 a(\mathbf{r}) + \left(1 + \frac{\delta\omega}{\omega_0}\right) 2ik_0 \frac{\partial}{\partial z'} a(\mathbf{r}) = 0, \tag{13.3.14}$$

which can alternatively be expressed as

$$\nabla_\perp^2 a(\mathbf{r}) + 2i\left(k_0 + \delta k\right) \frac{\partial}{\partial z'} a(\mathbf{r}) = 0 \tag{13.3.15}$$

where $\delta k = k_0\ (\delta\omega/\omega_0)$. This wave thus diffracts as a wave of frequency $\omega_0 + \delta\omega$ rather than a wave of frequency ω_0. More generally, for the case of an ultrashort pulse, the operator $\left[1 + (i/\omega_0)\partial/\partial\tau\right]$ describes the fact that different frequency components of the pulse diffract into different cone angles. Thus, after propagation, different frequency components will have different radial dependences. These effects and their implications for self-focusing have been described by Rothenberg (1992).

13.3.3 Supercontinuum Generation

When a short intense light pulse propagates through a nonlinear optical medium, it often undergoes significant spectral broadening. This process has since come to be known as supercontinuum generation (SCG). A particularly dramatic example of such behavior was reported by Alfano and Shapiro (1970), who observed broadening over much of the visible spectrum when laser pulses of 4 ps duration and 530 nm wavelength were focused into samples of calcite, quartz, sodium chloride, and several glasses. Self-focusing of the laser light to beam diameters of the order of 20 microns was observed to accompany the spectral broadening. SCG excited by femtosecond pulses has been observed by Fork et al. (1983). SCG has also been observed in gases Corkum et al. (1986).

The basic underlying mechanism of SCG is believed to be that of self-phase modulation, which was described earlier in subsection 7.5.1. Except for the case of SCG in optical fibers, SCG is found to occur primarily when it is accompanied by the breakup of the laser beam into small-scale filaments. The explosive increase in pulse intensity associated with self-focusing dramatically enhances the process of self-phase modulation, as well as other nonlinear processes such as self-steepening (Yang and Shen, 1984). Gaeta (2000) has emphasized that under conditions of catastrophic self-focusing the process of self-steeping leads to the formation of an optical shock wave on the trailing edge of the optical pulse which thereby leads to the generation of an extremely broad output spectrum.

13.4 Intense-Field Nonlinear Optics

Most nonlinear optical phenomena* can be described by assuming that the material polarization can be expanded as a power series in the applied electric field amplitude. This relation in its simplest form is given by

$$\tilde{P}(t) = \epsilon_0 \chi^{(1)} \tilde{E}(t) + \epsilon_0 \chi^{(2)} \tilde{E}(t)^2 + \epsilon_0 \chi^{(3)} \tilde{E}(t)^3 + \cdots . \tag{13.4.1}$$

However, for sufficiently large field strengths, this power series expansion does not converge. We saw in Chapter 6 that under resonant conditions this power-series description breaks down if the Rabi frequency $\Omega = \mu_{ba} E/\hbar$ associated with the interaction of the laser field with the atom becomes comparable to $1/T_1$, where T_1 is the atomic excited-state lifetime. However, the power-series description of Eq. (13.4.1) can become invalid even under highly nonresonant conditions. For example, this equation will certainly become invalid if the laser field amplitude E becomes comparable to or larger than the atomic field strength

$$E_{\text{at}} = \frac{e}{4\pi\epsilon_0 a_0^2} = \frac{e}{4\pi\epsilon_0 (4\pi\epsilon_0 \hbar^2/me^2)^2} = 6 \times 10^{11} \text{ V/m}, \tag{13.4.2}$$

which corresponds to a laser intensity of†

$$I_{\text{at}} = \tfrac{1}{2}\epsilon_0 c E_{\text{at}}^2 = 4 \times 10^{16} \text{ W/cm}^2 = 4 \times 10^{20} \text{ W/m}^2. \tag{13.4.3}$$

In fact, lasers that can produce intensities larger than 10^{20} W/cm^2 are presently available (see for instance Mourou et al., 1998). In the remainder of the present chapter we explore some of the physical phenomena that can occur through use of fields of such intensity. Additional information on this topic can be found for example in the review article of Brabec and Krausz (2000a).

Let us begin by considering briefly the conceptual framework one might use to describe intense-field nonlinear optics. Recall that the quantum-mechanical calculation of the nonlinear optical susceptibility presented in Chapter 3 presupposes that the Hamiltonian of an atom in the presence of a laser field is of the form

$$\hat{H} = \hat{H}_0 + \hat{V}(t), \tag{13.4.4}$$

where $\hat{H}_0$ is the Hamiltonian of an isolated atom and $\hat{V}(t) = -\mu \tilde{E}(t)$ represents the interaction energy of the atom with the laser field. Schrödinger's equation is then solved for this Hamiltonian through use of perturbation theory under the assumption $V(t) \ll H_0$. For the case of intense-field nonlinear optics, the nature of this inequality is the reverse—that is, the interaction energy $V(t)$ is much larger than H_0. This observation suggests that it should prove useful to begin our study of intense-field nonlinear optics by considering the motion of a free electron in an intense laser field.

* The photorefractive effect of Chapter 11 being an obvious exception.

† Here we take the *peak* field strength of the optical wave, which we assume to be linearly polarized, to be E_{at}.

13.5 Motion of a Free Electron in a Laser Field

Let us initially ignore both relativistic effects and the influence of the magnetic field associated with the laser beam. We assume the laser beam to be linearly polarized and of the form $\tilde{\mathbf{E}}(t) = \tilde{E}(t)\hat{x}$, where $\tilde{E}(t) = Ee^{-i\omega t} + \text{c.c.}$ The equation of motion of the electron is then given by

$$m\ddot{\tilde{x}} = -e\tilde{E}(t) \quad \text{or} \quad m\ddot{\tilde{x}} = -eEe^{-i\omega t} + \text{c.c.}, \tag{13.5.1}$$

which leads to the solution

$$\tilde{x}(t) = xe^{-i\omega t} + \text{c.c.}, \tag{13.5.2}$$

where

$$x = eE/m\omega^2. \tag{13.5.3}$$

The time-averaged kinetic energy associated with this motion is given by $K = \frac{1}{2}m\langle\dot{\tilde{x}}(t)^2\rangle$ or, since

$$\dot{\tilde{x}}(t) = (-i\omega x)e^{-i\omega t} + \text{c.c.}, \tag{13.5.4}$$

by

$$K = \frac{e^2E^2}{m\omega^2} = \frac{e^2E_0^2}{4m\omega^2}, \tag{13.5.5}$$

where E_0 denotes the peak value of the electric field of the laser illumination. This energy is known as the jitter energy or the quiver energy (as it is associated with the oscillation of the electron about its equilibrium position) or as the ponderomotive energy (Kibble, 1966). This energy can be appreciable. By way of example, consider a laser field of wavelength 1.06 μm. One finds by numerical evaluation that the ponderomotive energy is equal to 13.6 eV (a typical atomic energy) for $I = 1.3 \times 10^{14}$ W/cm^2 $= 1.3 \times 10^{18}$ W/m^2, is equal to 4.2 keV for $I = I_{\text{at}}$ (which is given by Eq. (13.4.3)), and is equal to $mc^2 = 500$ keV for $I = 4.8 \times 10^{18}$ W/cm^2 $= 4.8 \times 10^{22}$ W/m^2.

The equation of motion (13.5.1) and its solution (13.5.2) are linear in the laser field amplitude. Both magnetic and relativistic effects can induce nonlinearity in the electronic response. Let us consider briefly the influence of magnetic effects; see also Problem 1 at the end of this chapter for a more detailed analysis. The electric field of Eq. (13.5.1) has a magnetic field associated with it. Assuming propagation in the z direction, this magnetic field is of the form $\tilde{\mathbf{B}}(t) = \tilde{B}(t)\hat{y}$, where $\tilde{B}(t) = Be^{i\omega t} + \text{c.c.}$ and where, assuming propagation in vacuum, $B = E/c$. According to Eq. (13.5.4) the electron has a velocity in the x direction, and it will

thus will experience a magnetic force $\mathbf{F} = -e\mathbf{v} \times \mathbf{B}$ in the z direction. The equation of motion for the z component of the velocity is thus

$$m\ddot{z} = \left[\left(-\frac{ieE}{m\omega}\right)e^{-i\omega t} + \text{c.c.}\right]\left[Be^{-i\omega t} + \text{c.c.}\right]. \tag{13.5.6}$$

The right-hand side of this equation consists of terms at zero frequency and at frequencies $\pm 2\omega$. When Eq. (13.5.6) is solved, one finds that the z-component of the electron motion consists of oscillations at frequency 2ω and amplitude $eEB/m^2\omega^3$. This motion is superposed on a uniform drift velocity. The velocity associated with this oscillatory motion leads to a magnetic force in the x direction at frequency 3ω. In similar manner, all harmonics of the laser frequency appear in the atomic motion.*

As just noted, relativistic effects also lead to nonlinearities in the atomic response. The origin of this effect is the relativistic change in electron mass that occurs when the electron velocity becomes comparable to the speed of light c in vacuum. The resulting motion can be described in a relatively straightforward manner. Landau and Lifshitz (1960) show that for beam of peak field strength E_0, i.e., $\tilde{E}(t) = E_0 \cos(\omega t - \omega z/c)$, linearly polarized in the x-direction, the electron moves in a figure-8 pattern superposed on a uniform translational motion in the z-direction. In the reference frame moving with the uniform translational velocity, the electron motion can be described by the equations

$$x = \frac{\beta c}{\omega}\cos\eta, \qquad y = 0, \qquad z = \frac{\beta^2 c}{8\omega}\sin 2\eta, \tag{13.5.7}$$

where

$$\eta = \omega(t - z/c), \tag{13.5.8a}$$

$$\beta = eE_0/\gamma'\omega, \tag{13.5.8b}$$

$$\gamma'^2 = m^2c^2 + e^2E_0^2/2\omega^2. \tag{13.5.8c}$$

For circularly polarized radiation described by $E_x = E_0\cos(\omega t - \omega z/c)$, $E_y = E_0\sin(\omega t - \omega z/c)$, there is no induced drift velocity, and the electron moves with uniform angular velocity in a circle of radius $ecE_0/\gamma'\omega^2$; this motion can be described by the equations

$$x = \frac{\beta c}{\omega}\sin\omega t, \qquad y = \frac{\beta c}{\omega}\cos\omega t, \qquad z = 0, \tag{13.5.9}$$

where β has the same definition as above, but with $\gamma'^2 = m^2c^2 + e^2E_0^2/\omega^2$. These conclusions are summarized in Fig. 13.5.1. More detailed treatments of the motion of a free electron in a

* This conclusion arises, for instance, as a generalization of the results of Problem 7 of Chapter 4.

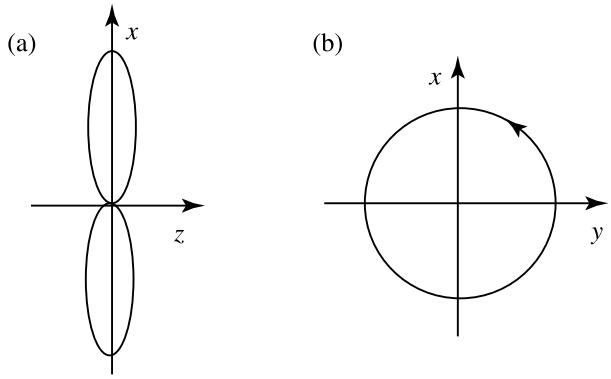

FIGURE 13.5.1: Motion of a free electron in (a) a linearly polarized laser field and (b) a circularly polarized field. Note that for linearly polarized light the motion is in the xz plane and that for circularly polarized light is in the xy plane.

laser field can be found in Sarachik and Schappert (1970) and in Castillo-Herrara and Johnston (1993).

It is convenient to introduce a dimensionless parameter a to quantify the strength of the applied laser field. This parameter can be interpreted as the Lorentz-invariant, dimensionless vector potential and is defined by the relation

$$a^2 = \frac{K}{mc^2} = \frac{e^2E^2}{m^2c^2\omega^2}. \tag{13.5.10}$$

This relation can also be expressed as

$$a^2 = \frac{1}{2\pi}\frac{Ir_0\lambda^2}{mc^3}, \tag{13.5.11}$$

where $r_0 = e^2/4\pi\epsilon_0 mc^2$ is the classical electron radius, $\lambda = 2\pi c/\omega$ is the vacuum wavelength of the laser radiation, and $I = 2\epsilon_0 cE^2$ is the laser intensity. The interpretation of the parameter a is that $a^2 \ll 1$ is the nonrelativistic regime, $a^2 \gtrsim 1$ is the relativistic regime, and $a^2 \gg 1$ is the ultrarelativistic regime.

13.6 High-Harmonic Generation

High-harmonic generation is a dramatic process in which an intense laser beam* illuminates an atomic medium and all odd harmonics $q\omega$ of the laser frequency ω up to some cutoff order

* Intense in the sense that the ponderomotive energy K is much larger than the ionization potential I_P.

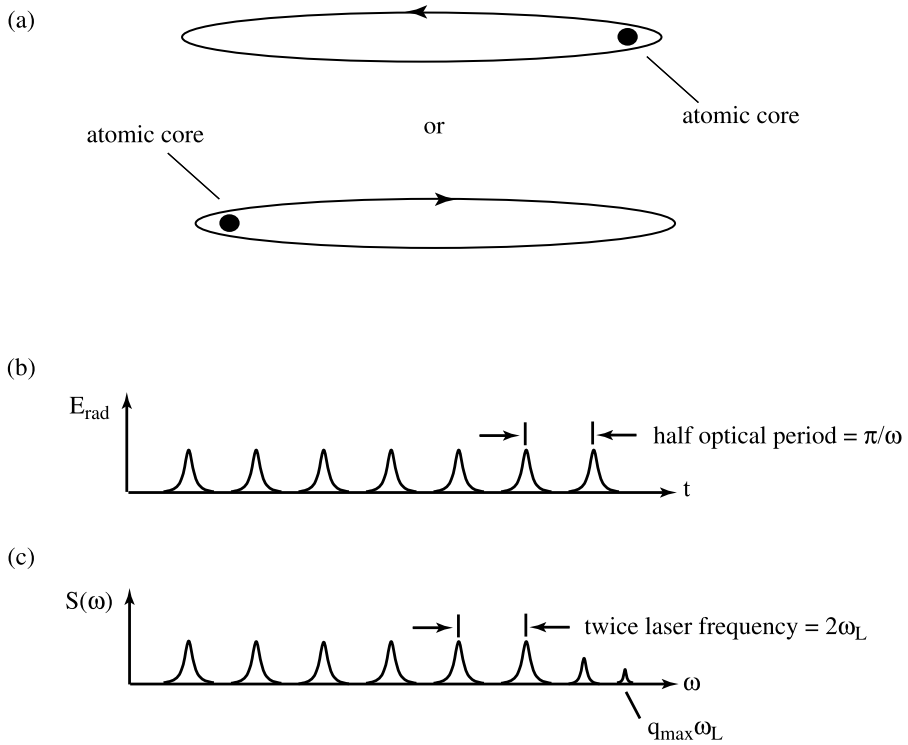

FIGURE 13.6.1: Corkum's model of high-harmonic generation. (a) Trajectory of an electron in the presence of a linearly polarized laser field of frequency ω with an intensity above the threshold for ionization. The electron emits a brief pulse of radiation each time it collides with the atomic core. The radiation from a collection of such electrons thus has the form shown in (b). The spectrum of the emitted radiation is determined by the square of the Fourier transform of this pulse train, and thus has the form shown in (c).

$q_{\max}$ are emitted in the forward direction. It is found that most of the harmonics are emitted with comparable efficiency. This observation demonstrates that high-harmonic generation is not a perturbative (i.e., is not a $\chi^{(q)}$) process. For a perturbative process, each successively higher order would be expected to be emitted with a smaller efficiency. Harmonic orders as large as $q = 221$ have been observed Chang et al. (1999). More recently, Popmintchev et al. (2012) reported high-harmonic generation from helium excited by 80-fsec pulses from an optical parametric chirped-pulse amplification system operating at 3.9 μm. They observed a coherent high-harmonic continuum reaching to 1.6 keV, corresponding to greater than the 5000th harmonic order. High-harmonic generation is typically observed using laser intensities in the range 10^{14}–10^{16} W/cm^2.

Many of the features of high-harmonic generation can be understood in terms of a model due to Corkum (1993). One imagines an atom in the presence of a linearly polarized laser field

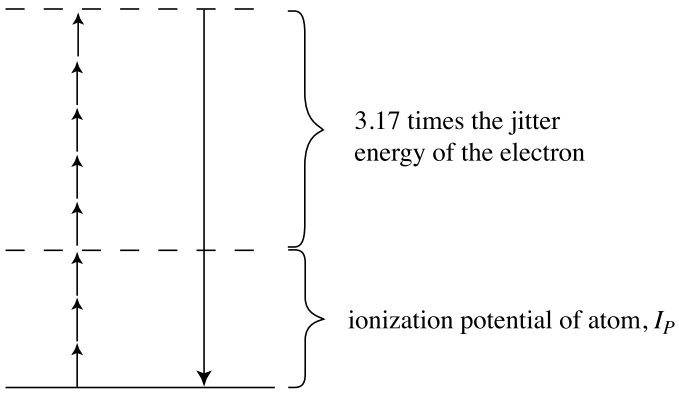

FIGURE 13.6.2: Schematic representation of the empirical relation $\hbar\omega q_{\max} = 3.17K + I_P$. The numerical factor of 3.17 is a consequence of detailed analysis of the dynamics of an electron interacting simultaneously with an external laser field and the atomic core.

sufficiently intense to ionize the atom. Even though the electron kinetic energy K might greatly exceed the ionization potential I_P of the atom, because of the oscillatory nature of the optical field the electron will follow an oscillatory trajectory that returns it to the atomic core once each optical period, as illustrated in Fig. 13.6.1. Because of the $1/r^2$ nature of the Coulomb potential, the electron will feel an appreciable force and thus an acceleration only when it is very close to the atomic core. The radiated field is proportional to the instantaneous acceleration, and the field radiated by any individual electron will thus consist of a sequence of pulses separated by the optical period of the fundamental laser field. However, in a collection of atoms, roughly half of the ejected electrons will be emitted near the positive maximum of the oscillating laser field and half near the negative maximum, and consequently the emitted radiation will consist of a sequence of pulses separated by half the optical period of the fundamental laser field. These pulses are mutually coherent, and thus the spectrum of the emitted radiation is the Fourier transform of this pulse train, which is a series of components separated by twice the laser frequency. Thus only odd harmonics are emitted, in consistency with the general symmetry properties of centrosymmetric material media, as described in Section 1.5.

Arguments based on energetics can be used to estimate the maximum harmonic order $q_{\max}$. The process of high-harmonic generation is illustrated symbolically in Fig. 13.6.2. The energy available to the emitted photon is the sum of the available kinetic energy of the electron less the (negative) ionization energy of the atom. This line of reasoning might suggest $q_{\max}\hbar\omega = K + I_P$, but detailed calculations show that the coefficient of the kinetic energy term is in fact 3.17, so

$$q_{\max}\hbar\omega = 3.17K + I_P. \tag{13.6.1}$$

This prediction is in good agreement with laboratory data.

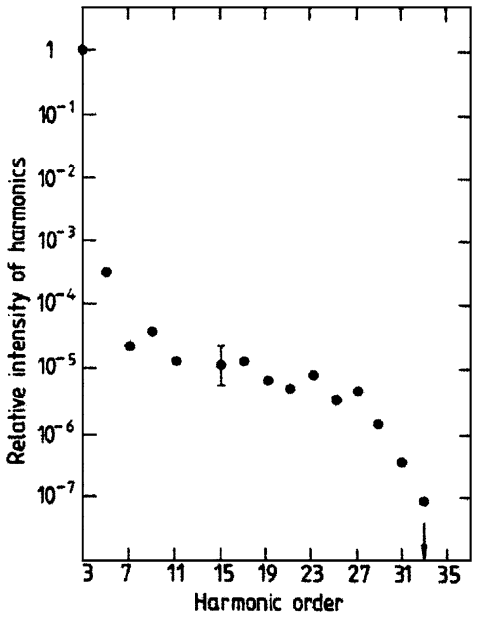

FIGURE 13.6.3: Experimental data of Ferray et al. (1988) illustrating high-harmonic generation.

We conclude this section with a brief historical summary of progress in the field of intense-field nonlinear optics and high-harmonic generation. Agostini et al. (1979) reported the observation of a phenomenon that has come to be called above-threshold ionization (ATI). This group measured the energy spectra of electrons produced by photoionization and observed multiple peaks separated by the photon energy $\hbar\omega$. This observation attracted great theoretical interest because, according to then-current theoretical models based on lowest-order perturbation theory, only one peak associated with the minimum number of photons needed to produce ionization was expected to be present. More recent work has included the possibility of double ionization in which two electrons are ejected as part of the photoionization process (Walker et al., 1994). One of the earliest observations of high-harmonic generation was that of Ferray et al. (1988), who observed up to the 33rd harmonic with laser intensities as large as 10^{13} W/cm^2 using Ar, Kr, and Xe gases (Fig. 13.6.3). Kulander and Shore (1989) presented one of the first successful computer models of high-harmonic generation. L'Huillier and Balcou (1993) observed HHG using pulses of 1 psec duration and intensities as large as 10^{15} W/cm^2, and observed harmonics up to the 135th order in Ne. Corkum (1993) presented the theoretical model of HHG described in the previous two paragraphs. Nearly simultaneously, Schafer et al. (1993) presented similar ideas along with experimental data. Lewenstein et al. (1994) presented a fully quantum-mechanical theory of HHG that clarified the underlying physics and produced quantitative predictions. They find that under certain assumptions the coefficient of I_p

in Eq. (13.6.1) should be 1.32 rather than unity. Chang et al. (1997) reported HHG in He excited by 26-fsec laser pulses from a Ti : sapphire laser system operating at 800 nm. They observed harmonic peaks up to a maximum of the 221st order and unresolved structure up to an energy (460 eV or 2.7 nm wavelength) corresponding to the 297th order. Slightly shorter wavelengths ($\lambda = 2.5$ nm, $h\nu = 500$ eV) have been observed by Schnürer et al. (1998). Durfee et al. (1999) have shown how to phase match the process of HHG by propagating the laser beam through a gas-filled capillary waveguide. Ghimire et al. (2011) reported the surprising observation of HHG in a crystalline solid. Until that time, it had been assumed that the electron collision rate in a solid would be too large to allow the occurrence of HHG. A theoretical explanation for this result has been presented by Vampa et al. (2014).

13.7 Tunnel Ionization and the Keldysh Model

There are two distinct processes that can lead to photoionization of an atom or molecule. One process is multiphoton ionization. This process is analogous to the process of multiphoton absorption that we studied earlier, with the crucial distinction that in multiphoton absorption the final state is a bound state of the electron, whereas in multiphoton ionization the final state is a free state. This behavior is illustrated in part (a) Fig. 13.7.1.

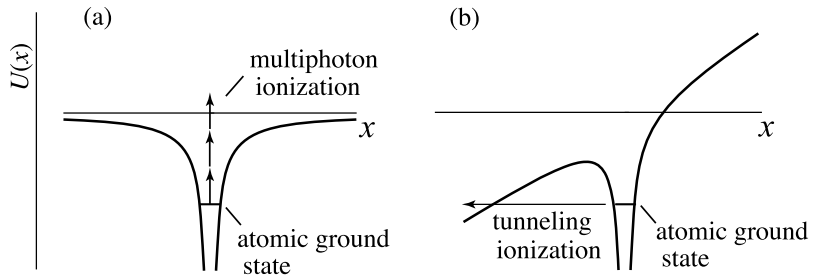

FIGURE 13.7.1: Two processes of photoionization. (a) Multiphoton ionization. (b) Tunnel ionization.

The other process is tunnel ionization, as illustrated in part (b) of this figure. This process occurs when the electric field of the laser light is sufficiently strong to significantly modify the Coulomb potential that binds the electron to the positively charged atomic core. The nature of the modification of the atomic binding in the presence of a strong laser field is illustrated in Fig. 13.7.2.

Keldysh (1965) showed that there is a quantity now known as the Keldysh parameter γ_K that determines which of the two process dominates. Specifically, multiphoton ionization dominates for $\gamma_K > 1$ and tunneling ionization dominates for $\gamma_K < 1$. The Keldysh parameter is given by

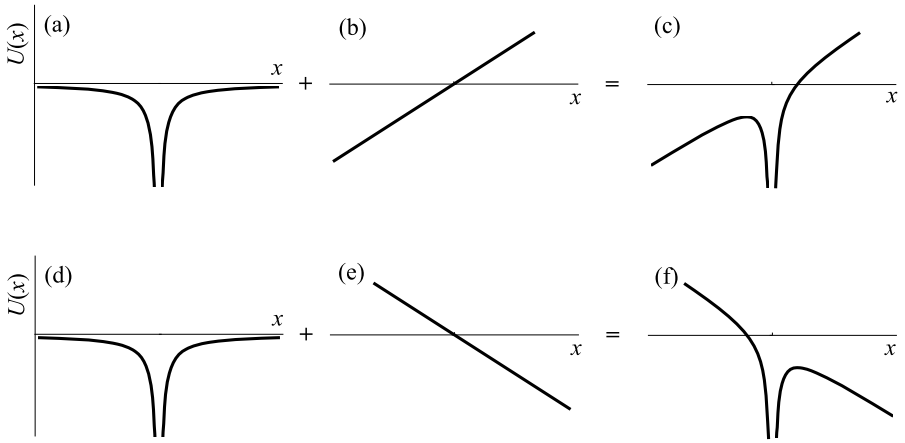

FIGURE 13.7.2: (a) The coulomb potential that binds the electron to the atomic core. (b) At a given moment of time, the electric field of the applied laser field produces a potential of the form shown. (c) The total potential is the sum of the Coulomb and the laser contributions. (d) through (f) At a half cycle later of the laser period, the potential is inverted in sign leading to the total potential shown in (f).

either of the two expressions (Brabec and Krausz, 2000b)

$$\gamma_K = \frac{eE}{\omega_L \sqrt{2mI_P}} = \sqrt{I_P/2K} \tag{13.7.1}$$

where ω_L is the laser frequency, m is the effective electron mass, I_P is the ionization potential of the atom, and K is the ponderomotive energy of Eq. (13.5.5). The Keldysh parameter can be given by the equivalent expression (Lenzer and Rudolph, 2008)

$$\gamma_K = \omega\tau = (\omega_L/|eE|)\sqrt{m_r I_P} \tag{13.7.2}$$

Refinements to the Keldysh model have been presented by other workers, and in particular by Ammosov et al. (1986).

13.8 Nonlinear Optics of Plasmas and Relativistic Nonlinear Optics

A plasma is a partially or fully ionized gas. Plasmas play an important role in nonlinear optics in two different ways: (1) Nonlinear optical processes such as multiphoton ionization can create a plasma. The optical properties of the material system are thereby modified even by the linear response of the plasma. (2) A plasma (no matter how it is generated) can respond in an intrinsically nonlinear manner to an applied optical field. In the present section we briefly survey both sorts of nonlinear optical response.

Let us first consider the process of plasma formation. We let N_e denote the number of free electrons per unit volume and N_i the corresponding number of positive ions. We also let N_T denote the total number of atoms present, both ionized and un-ionized. We assume that these quantities obey the rate equation

$$\frac{dN_e}{dt} = \frac{dN_i}{dt} = (N_T - N_i)\sigma^{(N)} I^N - r N_e N_i. \tag{13.8.1}$$

Here $\sigma^{(N)}$ is the N-photon absorption cross section (see also Section 12.5) and r is the electron–ion recombination rate. For short laser pulses of the sort often used to study plasma nonlinearities, recombination is an unlikely event and the last term in this equation can usually be ignored. In this case, the electron density increases monotonically during the laser pulse.

Let us next consider the (linear) optical properties of a plasma. We found above (Eqs. (13.5.2) and (13.5.3)) that the position of an electron in the field $\tilde{E}(t) = Ee^{-i\omega t} + \text{c.c.}$ will vary according to $\tilde{x}(t) = xe^{-i\omega t} + \text{c.c.}$ where $x = eE/m\omega^2$. The dipole moment associated with this response is $\tilde{p}(t) \equiv pe^{-i\omega t} + \text{c.c.} = -e\tilde{x}(t)$. The polarizability $\alpha(\omega)$ defined by $p = \epsilon_0 \alpha(\omega) E$ is thus given by

$$\alpha(\omega) = -\frac{e^2}{\epsilon_0 m\omega^2}. \tag{13.8.2}$$

The dielectric constant of a collection of such electrons is thus given by

$$\epsilon = 1 + N\alpha(\omega) = 1 - \frac{Ne^2}{\epsilon_0 m\omega^2}, \tag{13.8.3}$$

which is often expressed as

$$\epsilon = 1 - \frac{\omega_p^2}{\omega^2}, \quad \text{where} \quad \omega_p^2 = \frac{Ne^2}{\epsilon_0 m} \tag{13.8.4}$$

and where ω_p is known as the plasma frequency. For N sufficiently small that $\omega_p^2 < \omega^2$ (known as an underdense plasma), the dielectric constant is positive, $n = \sqrt{\epsilon}$ is real, and light waves can propagate. Conversely, for N sufficiently large that $\omega_p^2 > \omega^2$ (an overdense plasma), the dielectric constant is negative, $n = \sqrt{\epsilon}$ is imaginary, and light waves cannot propagate.

By way of comparison, we recall that for a bound electron the linear polarizability is given (see Eq. (1.4.17) and note that $\chi^{(1)}(\omega) = N\epsilon_0\alpha(\omega)$) by

$$\alpha(\omega) = \frac{e^2/m\epsilon_0}{\omega_0^2 - \omega^2 - 2i\omega\gamma}, \tag{13.8.5}$$

which in the highly nonresonant limit $\omega \ll \omega_0$ reduces to

$$\alpha_{\text{bound}} = \frac{e^2}{\epsilon_0 m\omega_0^2}. \tag{13.8.6}$$

Note that the polarizability of a free electron is opposite in sign and (for the common situation $\omega \ll \omega_0$) much larger in magnitude than that of a bound electron. Thus the process of plasma formation creates a large *negative* contribution to the refractive index. Note also that we have ignored the contribution of the ionic core to the polarizability because it is very much smaller than the electronic contribution, because the mass of the ion is much larger than that of the electron.

Let us next consider nonlinear optical effects that occur within a plasma. There are two primary mechanisms of nonlinearity: (1) ponderomotive effects and (2) relativistic effects.

Ponderomotive effects result from the tendency of polarizable particles to be expelled from regions of high field strength. These effects are particularly important for laser pulses sufficiently long in duration for particle motion to be important. Ponderomotive effects share an identical origin with the electrostrictive effects described in Section 9.2; the effect is simply given a different name in the context of plasma nonlinearities. Despite the fact that $\alpha(\omega)$ is negative for a free electron (the ponderomotive case) but positive for bulk matter (the electrostrictive case), both effects lead to an increase in refractive index. In the ponderomotive case, the electron, which makes a negative contribution to the refractive index, is expelled from the laser beam, leading to an increase in refractive index.

Another mechanism of nonlinearity in plasmas is provided by relativistic effects (Wagner et al., 1997). In a sufficiently intense laser beam ($I \gtrsim 10^{20}$ W/m^2) a free electron can be accelerated to relativistic velocities in a half optical period $T/2$. To demonstrate this result, we first calculate the electric field strength E_{rel} required to accelerate an electron to a velocity v comparable to c in a time $t = T/2 = \pi/\omega$. We thus set c equal to the acceleration (eE_{rel}/m) times $t = (\pi/\omega)$, from which we find that

$$E_{\text{rel}} = \frac{2mc^2}{\lambda e} \tag{13.8.7}$$

where $\lambda = 2\pi c/\omega$. For a vacuum wavelength of 1 μm, this field strength is equal to 1.0×10^{12} V/m. The optical intensity $I_{\text{rel}} = \frac{1}{2}\epsilon_0 c E_{\text{rel}}^2$ associated with this peak field strength is of the order of 10^{20} W/m^2 at a vacuum wavelength of 1 μm.

In analyzing the nonlinear response of an electron plasma, both ponderomotive and relativistic effects must be taken into account. However, the treatment simplifies considerably for the case of a linearly polarized excitation field because of a fortuitous cancellation of two of the contributions to the nonlinear response (Sprangle et al., 1987). The surviving contribution is the time-averaged change in electron mass due to relativistic effects. We next treat this contribution in detail.

Even when the electron velocity v is considerably smaller than velocity of light in vacuum c, appreciable nonlinear effects can be induced by the relativistic change in the electron mass, that is, the change in electron mass from m to γm where

$$\gamma = \frac{1}{\sqrt{1 - v^2/c^2}}. \tag{13.8.8}$$

The value of the plasma frequency and consequently the refractive index of the plasma is thereby modified such that

$$n^2 = 1 - \frac{\omega_p^2}{\gamma\omega^2}, \tag{13.8.9}$$

where as before $\omega_p^2 = Ne^2/\epsilon_0 m$. Detailed analysis (Max et al., 1974; Sprangle et al., 1987) shows that the value of the relativistic factor γ to be used in Eq. (13.8.9) is given in general (that is, even in the strongly relativistic limit) by the expression

$$\gamma^2 = 1 + \frac{e^2 E_0^2}{m^2\omega^2 c^2}, \tag{13.8.10}$$

where E_0 is the peak field amplitude of the incident laser field. In writing this result in the form shown, we have assumed that the transverse contribution to the velocity is much larger than the longitudinal component.

We next calculate the nonlinear coefficient n_2 by determining the lowest-order change in refractive index. The relativistic factor γ is given by the square root of expression (13.8.10), which to lowest order becomes

$$\gamma = 1 + \frac{1}{2}\frac{e^2 E_0^2}{m^2\omega^2 c^2} \equiv 1 + x, \tag{13.8.11}$$

where the parameter x has been introduced for future convenience. We can thus write Eq. (13.8.9) as

$$\begin{aligned} n^2 &= 1 - \frac{\omega_p^2}{\omega^2(1+x)} \simeq 1 - \frac{\omega_p^2}{\omega^2}(1-x) \\ &= n_0^2 + \frac{\omega_p^2}{\omega^2}x, \end{aligned} \tag{13.8.12}$$

where $n_0^2 = 1 - \omega_p^2/\omega^2$. We can thus express n as

$$n \simeq n_0 + \frac{1}{2n_0}\frac{\omega_p^2}{\omega^2}x \equiv n_0 + n_2 I. \tag{13.8.13}$$

Setting I equal to $\frac{1}{2}n_0\epsilon_0 c E_0^2$, we find that

$$n_2 = \frac{\omega_p^2 e^2}{2n_0^2\epsilon_0 m^2 c^3 \omega^4}. \tag{13.8.14}$$

This expression gives the relativistic contribution to the nonlinear refractive index. Note that this process is purely relativistic: Planck's constant does not appear in this expression. Note further that expression (13.8.14) can be rewritten in the intuitively revealing form

$$n_2 = \frac{1}{2\pi n_0^2}\left(\frac{\omega_p}{\omega}\right)^2\left[\frac{\lambda^2}{(mc^2)/(r_0/c)}\right], \tag{13.8.15}$$

where $\lambda = 2\pi c/\omega$ and $r_0 = e^2/4\pi\epsilon_0 mc^2 = 2.6 \times 10^{-15}$ m is the classical electron radius. The term in square brackets can be interpreted as the fundamental relativistic unit of nonlinear refractive index, that is, an area (λ^2) divided by the fundamental unit of power P_{rel} (the electron rest mass mc^2 divided by the transit time of light across the classical radius of the electron). Numerically we find that

$$P_{\text{rel}} = \frac{mc^2}{(r_0/c)} = \frac{(0.5 \times 10^6)(1.6 \times 10^{-19})}{(2.6 \times 10^{-15}/3 \times 10^8)} = 9.2 \times 10^9 \text{ W}. \tag{13.8.16}$$

At a wavelength of $\lambda = 1$ μm, one thus finds that

$$n_2 = \frac{1}{2\pi n_0^2}\left(\frac{\omega_p}{\omega}\right)^2\left(\frac{10^{-12}}{9.2 \times 10^9}\right) = \frac{1}{2\pi n_0^2}\left(\frac{\omega_p}{\omega}\right)^2 1.1 \times 10^{-22}\ \frac{\text{m}^2}{\text{W}}. \tag{13.8.17}$$

On the basis of the expression for n_2 just derived, one can calculate the critical power for self-focusing in a plasma. Since in general the expression for the critical power is given by Eq. (7.1.10) as

$$P_{\text{cr}} = \frac{(0.61)^2\pi\lambda^2}{8n_0 n_2} \simeq \frac{\lambda^2}{8n_0 n_2}, \tag{13.8.18}$$

we find through use of Eq. (13.8.14) that

$$P_{\text{cr}} = \frac{\pi}{4}n_0 c\left(\frac{mc^2}{e}\right)^2\left(\frac{\omega}{\omega_p}\right)^2 = 6.7\left(\frac{\omega}{\omega_p}\right)^2 \text{ GW}. \tag{13.8.19}$$

An expression for the critical power was first derived by Sprangle et al. (1987) using slightly different assumptions, yielding a similar expression but with the factor $(\pi/4)$ in the first form replaced by 2 and thus the numerical factor 6.7 in the second form replaced by 17. Relativistic self-focusing has been observed experimentally by Monot et al. (1995). Note further that Eq. (13.8.19) can be reexpressed in the suggestive form

$$P_{\text{cr}} = \frac{\pi}{4}n_0\left(\frac{\omega}{\omega_p}\right)^2\left(\frac{mc^2}{r_0/c}\right). \tag{13.8.20}$$

Here, as in Eq. (13.8.16), the last factor denotes the relativistic unit of optical power.

13.9 Nonlinear Quantum Electrodynamics

We saw in Eq. (13.8.7) that there is a characteristic field strength $E_{\text{rel}} = 2mc^2/e\lambda$ for light of vacuum wavelength λ at which relativistic effects become important. There is another field strength E_{QED} at which effects associated with the quantum vacuum become important. This field strength is defined by the relations

$$E_{\text{QED}} = \frac{m^2c^3}{e\hbar} = \frac{mc^2}{e\lambda\!\!\!^{-}_{\text{C}}}, \quad \text{where} \quad \lambda\!\!\!^{-}_{\text{C}} = \frac{\hbar}{mc}. \tag{13.9.1}$$

Here $\lambda\!\!\!^{-}_{\text{C}} = 3.6 \times 10^{-11}$ cm $= 3.6 \times 10^{-13}$ m is the (reduced) Compton wavelength of the electron. The Compton wavelength is one measure of the size of the electron in the sense that the position of the electron cannot be localized to an accuracy better than $\lambda\!\!\!^{-}_{\text{C}}$.* The QED field strength is thus a measure of the field strength required to accelerate an electron to relativistic velocities in a distance of the order of the size of the electron. Consequently a field of this magnitude is large enough to lead to the spontaneous creation of electron–positron pairs.

The QED field strength is given numerically by

$$E_{\text{QED}} = 1.32 \times 10^{16} \text{ V/cm} = 1.32 \times 10^{18} \text{ V/m}. \tag{13.9.2}$$

This field strength is often referred to as the Schwinger limit. The intensity of a wave whose peak field amplitude is equal to E_{QED} is consequently

$$I_{\text{QED}} = \tfrac{1}{2}\epsilon_0 c E_{\text{QED}}^2 = 4 \times 10^{29} \text{ W/cm}^2 = 4 \times 10^{33} \text{ W/m}^2. \tag{13.9.3}$$

This value exceeds the intensity that can be produced by the most powerful lasers currently available. From a different perspective, I_{QED} designates the largest laser intensity that could possibly be produced, in that a laser field of any larger intensity would be immediately absorbed as the result of electron–positron creation. Nonetheless, in the rest frame of a relativistic electron of energy W, produced, for example, by a particle accelerator, the intensity of a laser beam is greatly increased by relativistic effects. This increase occurs because the electric field strength in the electron rest frame is larger than the field in the laboratory frame by the factor $\gamma = W/mc^2$. In fact, electron–positron pair creation resulting from the interaction of a relativistic electron with a laser beam has been observed experimentally (Burke et al., 1997).

Nonlinear quantum electrodynamic effects have been predicted even for field strengths considerably smaller than E_{QED}. Euler and Kockel (1935) have shown that there is an intrinsic

* This conclusion follows as a consequence of the time–energy uncertainty relation, which we take in the form $\Delta E \Delta t \gtrsim \hbar$. We take the energy uncertainty to be the rest energy of an electron $\Delta E = mc^2$, and we set the time uncertainty to $\Delta t = \Delta x/c$. We thus find that the minimum uncertainty in position is $\Delta x = \hbar/mc$; we take this length as the definition of the reduced Compton wavelength $\lambda\!\!\!^{-}_{\text{C}}$. This result can be understood more intuitively by noting that a photon of wavelength shorter than $\sim\lambda\!\!\!^{-}_{\text{C}}$ would have an energy sufficiently large to create an electron–positron pair, thus rendering moot the question of the location of the original electron.

nonlinearity to the electromagnetic vacuum that leads to a field-dependent dielectric tensor of the form

$$\epsilon_{ik} = \delta_{ik} + \left(\frac{e^2}{4\pi\epsilon_0}\right)^2 \frac{\hbar}{45\pi m^4 c^7}\left[2\left(E^2 - B^2c^2\right)\delta_{ik} + 7B_iB_kc^2\right]. \tag{13.9.4}$$

This equation has been converted to SI units from the equation in its original published form. Note that the term containing $(E^2 - B^2c^2)$ vanishes for electromagnetic plane waves in vacuum, because of the relation $|\mathbf{E}| = |\mathbf{B}|c$. The dielectric response relevant to plane-wave laser beams is thus

$$\epsilon_{ik} = \delta_{ik} + \left(\frac{e^2}{4\pi\epsilon_0}\right)^2 \frac{7\hbar}{45\pi m^4 c^7} B_iB_kc^2, \tag{13.9.5}$$

which can be expressed through use of Eq. (13.9.1) as

$$\epsilon_{ik} = \delta_{ik} + \frac{7}{45\pi}\left(\frac{e^2}{4\pi\epsilon_0\hbar c}\right)\frac{B_iB_kc^2}{E_{\text{QED}}^2}. \tag{13.9.6}$$

Since the magnetic field (rather than the electric field) appears in the expression for the dielectric response, the tensor properties of the nonlinearity of the vacuum are different from those of typical optical nonlinearities. Nonetheless, by suppressing the tensor nature of the response, we can describe the nonlinearity in terms of a standard third-order susceptibility, and such a description is useful for comparing the size of this effect with that of other nonlinear optical processes. To proceed, we define the (scalar) change in dielectric constant as

$$\Delta\epsilon = \frac{7}{45\pi}\left(\frac{e^2}{4\pi\epsilon_0\hbar c}\right)\frac{B^2c^2}{E_{\text{QED}}^2} \tag{13.9.7}$$

and equate this quantity with $\chi^{(3)}E^2$, with the identification of B with E/c. We thus find that

$$\chi^{(3)} = \frac{7}{45\pi}\left(\frac{e^2}{4\pi\epsilon_0\hbar c}\right)\frac{1}{E_{\text{QED}}^2} \tag{13.9.8}$$

or, through use of Eq. (13.9.2) that

$$\chi^{(3)} = \frac{7}{45\pi}\frac{1}{137}\frac{1}{E_{\text{QED}}^2} = 2.1 \times 10^{-39}\ \text{m}^2/\text{V}^2. \tag{13.9.9}$$

We can express this result in terms of an intensity-dependent refractive index through use of Eq. (4.1.20), and find that

$$n_2 = 5.9 \times 10^{-37}\ \text{m}^2/\text{W}. \tag{13.9.10}$$

Recall, for comparison, that for silica glass $n_2 = 3.2 \times 10^{-20}$ m^2/W. Recall further that strong self-action effects are expected only if the power of a laser beam exceeds the critical power for self-focusing (Eq. (7.1.10))

$$P_{\rm cr} = \frac{\lambda^2}{8 n_0 n_2}. \tag{13.9.11}$$

We find by combining Eqs. (13.9.10) and (13.9.11) that at a wavelength of 1 μm,

$$P_{\rm cr} = 2.1 \times 10^{23} \text{ W}, \tag{13.9.12}$$

which is considerably larger than the power of any laser source currently contemplated.

Problem

1. Consider the nonrelativistic motion of a free electron in the laser field $\tilde{\mathbf{E}}(z,t) = E_0 \cos \omega t \, \hat{\mathbf{x}}$, $\tilde{\mathbf{B}}(z,t) = B_0 \cos \omega t \, \hat{\mathbf{y}}$ with $B_0 c = E_0$. Assume that the electron is injected into the field at rest at position $x = 0$, $y = 0$ at time t_0.
   (a) Solve the equation of motion for the electron and thereby determine $x(t)$, $y(t)$, $z(t)$, $v_x(t)$, $v_y(t)$, and $v_z(t)$ for all $t > t_0$. Plot the trajectory of the electron of the electron motion, both in the laboratory frame and in a reference frame in which the electron is on average at rest (specify what frame this is). Note that some of these results depend on the value of t_0; for those that do, show plots for several different values of t_0.
   (b) Ignoring the magnetic contribution, calculate the peak and time-averaged kinetic energy of the electron.
   (c) Repeat for circular polarization.

References

Sections 13.1 through 13.3: Ultrafast Nonlinear Optics

Alfano, R.R., Shapiro, S.L., 1970. Phys. Rev. Lett. 24, 592.
Brabec, T., Krausz, F., 1997. Phys. Rev. Lett. 78, 3282.
Corkum, P.B., Rolland, C., Srinivasan-Rao, T., 1986. Phys. Rev. Lett. 57, 2268.
DeMartini, F., Townes, C.H., Gustafson, T.K., Kelley, P.L., 1967. Phys. Rev. 164, 312.
Diels, J.-C., Rudolph, W., 1996. Ultrashort Laser Pulse Phenomena. Academic Press, San Diego.
Fork, R.L., Shank, C.V., Hirlimann, C., Yen, R., Tomlinson, W.J., 1983. Opt. Lett. 8, 1.
Gaeta, A.L., 2000. Phys. Rev. Lett. 84, 3582.
Hentschel, M., Kienberger, R., Spielmann, Ch., Reider, G.A., Milosevic, N., Brabec, T., Corkum, P., Heinzmann, U., Drescher, M., Krausz, F., 2001. Attosecond metrology. Nature 414, 509.
Rothenberg, J.E., 1992. Opt. Lett. 17, 1340.
Yang, G., Shen, Y.R., 1984. Opt. Lett. 9, 510.

Sections 13.4 and 13.5: Intense-Field Nonlinear Optics and Motion of a Free Electron

Brabec, T., Krausz, F., 2000a. Rev. Mod. Phys. 72, 545.
Castillo-Herrara, C.I., Johnston, T.W., 1993. IEEE Trans. Plasma Sci. 21, 125.
Kibble, T.W.B., 1966. Phys. Rev. Lett. 16, 1054.
Landau, L.D., Lifshitz, E.M., 1960. Classical Theory of Fields. Pergamon Press, Oxford, Section 48.
Mourou, G.A., Barty, C.P.J., Perry, M.D., 1998. Phys. Today 51, 22.
Sarachik, E.S., Schappert, G.T., 1970. Phys. Rev. D 1, 2738.

Section 13.6: High-Harmonic Generation

Agostini, P., Fabre, F., Mainfray, G., Petite, G., Rahman, N.K., 1979. Phys. Rev. Lett. 42, 1127.
Chang, Z., Rundquist, A., Wang, H., Murnane, M.M., Kapteyn, H.C., 1997. Phys. Rev. Lett. 79, 2967.
Chang, Z., Rundquist, A., Wang, H., Murnane, M.M., Kapteyn, H.C., 1999. Phys. Rev. Lett. 82, 2006.
Corkum, P.B., 1993. Phys. Rev. Lett. 71, 1994.
Durfee III, C.G., Rundquist, A.R., Backus, S., Herne, C., Murnane, M.M., Kapteyn, H.C., 1999. Phys. Rev. Lett. 83, 2187.
Ferray, M., L'Huillier, A., Li, X.F., Lompre, L.A., Mainfray, G., Manus, C., 1988. J. Phys. B 21, L31.
Ghimire, S., DiChiara, A.D., Sistrunk, E., Agostini, P., DiMauroand, L.F., Reis, D.A., 2011. Nat. Phys. 7, 138–141.
Kulander, K.C., Shore, B.W., 1989. Phys. Rev. Lett. 62, 524.
Lewenstein, M., Balcou, Ph., Ivanov, M.Yu., L'Huillier, A., Corkum, P.B., 1994. Phys. Rev. A 49, 2117.
L'Huillier, A., Balcou, Ph., 1993. Phys. Rev. Lett. 70, 774.
Popmintchev, T., Murnane, M.M., Kapteyn, H.C., et al., 2012. Bright coherent ultrahigh harmonics in the keV X-ray regime from mid-infrared femtosecond lasers. Science 336, 1287.
Schnürer, M., Spielmann, Ch., Wobrauschek, P., Streli, C., Burnett, N.H., Kan, C., Ferencz, K., Koppitsch, R., Cheng, Z., Brabec, T., Krausz, F., 1998. Phys. Rev. Lett. 80, 3236.
Schafer, K.J., Yang, B., DiMauro, L.F., Kulander, K.C., 1993. Phys. Rev. Lett. 70, 1599.
Vampa, G., McDonald, C.R., Orlando, G., Klug, D.D., Corkum, P.B., Brabec, T., 2014. Theoretical analysis of high-harmonic generation in solids. Phys. Rev. Lett. 113, 073901.
Walker, B., Sheely, B., DiMauro, L.F., Agostini, P., Schafer, K.J., Kulander, K.C., 1994. Phys. Rev. Lett. 73, 1127.

Section 13.7: Tunnel Ionization and the Keldysh Mechanism

Ammosov, M.V., Delone, N.B., Krainov, V.P., 1986. Sov. Phys. JETP 64, 1191.
Brabec, T., Krausz, F., 2000b. Rev. Mod. Phys. 72, 545. See especially Eq. (21).
Keldysh, L.V., 1965. Sov. Phys. JETP 20, 1307.
Lenzer, M., Rudolph, W., 2008. In: Brabec, T. (Ed.), Strong Field Physics. Springer, New York. See especially p. 248.
Max, C.E., Arons, J., Langdon, A.B., 1974. Phys. Rev. Lett. 33, 209.
Monot, P., Auguste, T., Gibbon, P., Jakober, F., Mainfray, G., Dulieu, A., Louis-Jacquet, M., Malka, G., Miquel, J.L., 1995. Phys. Rev. Lett. 74, 2953.
Sprangle, P., Tang, C.-M., Esarez, E., 1987. IEEE Trans. Plasma Sci. 15, 145.
Wagner, R., Chen, S.-Y., Maksemchak, A., Umstadter, D., 1997. Phys. Rev. Lett. 78, 3125.

Section 13.9: Nonlinear Quantum Electrodynamics

Burke, D.L., Field, R.C., Horton-Smith, G., Spencer, J.E., Walz, D., Berridge, S.C., Bugg, W.M., Shmakov, K., Weidemann, A.W., Bula, C., McDonald, K.T., Prebys, E.J., Bamber, C., Boege, S.J., Koffas, T., Kotseroglou, T., Melissinos, A.C., Meyerhofer, D.D., Reis, D.A., Ragg, W., 1997. Phys. Rev. Lett. 79, 1626.
Euler, H., Kockel, K., 1935. Naturwissenschaften 23, 246.